

# Phase transitions induced on hexagonal manganites by the incorporation of aliovalent cations on A or B lattice sites

C. MOURE, D. GUTIÉRREZ, J.F. FERNÁNDEZ, J. TARTAJ, P. DURÁN y O. PENA<sup>1</sup>

Instituto de Cerámica y Vidrio, CSIC, Electrocerámics Departament 28500 Arganda del Rey, Madrid, Spain

<sup>1</sup>LCSIM, UMR 6511, Université de Rennes 1. FRANCIA

The phase transition to perovskite-type structure, that occurs in some hexagonal manganites when foreign cations are incorporated into solid solution, has been studied. Several solid solution series belonging to the  $Y(Mn, Ni)O_3$ ,  $(Er, Ca)MnO_3$ ,  $(Y, Ca)MnO_3$ , systems have been prepared by solid state reaction between the corresponding oxides. The crystalline structure of the different solid solutions has been established. The behaviour of the  $(Gd, Ca)MnO_3$  system has been taken as a reference. The obtained results are discussed as a function of the tolerance factor and the  $Mn^{3+}/Mn^{4+}$  ratio. The transition to perovskite structure is governed by this  $Mn^{3+}/Mn^{4+}$  ratio rather than the increase of the tolerance factor

*Keywords: lanthanide manganites, solid solutions, phase transitions*

## Transiciones de Fase introducidas en manganitas hexagonales por la incorporación de cationes aliovalentes en lugares A ó B.

Se ha estudiado la transición de fase a estructura de tipo perovskita que ocurre en algunas manganitas hexagonales cuando se incorporan iones aliovalentes formando soluciones sólidas. Se han preparado soluciones sólidas pertenecientes a los sistemas  $Y(Mn, Ni)O_3$ ,  $(Er, Ca)MnO_3$ ,  $(Y, Ca)MnO_3$  por reacción en estado sólido entre los óxidos. Se ha determinado la estructura cristalina de los diferentes compuestos, y los resultados se comparan con los observados en los correspondientes al sistema  $(Gd, Ca)MnO_3$ . Los resultados se discuten en función del factor de tolerancia y de la razón  $Mn^{3+}/Mn^{4+}$ . La transición es gobernada por dicha razón más bien que por la variación del factor de tolerancia

*Palabras clave: manganitas de tierras raras, soluciones sólidas, transiciones de fase.*

## 1. INTRODUCTION

Perovskite-type double oxides of rare earth and manganese cations are used as high temperature electrodes due to their high electrical conductivity and stability in the presence of  $O_2$  at relatively high temperatures (1). The  $LaMnO_3$  compound has widely studied as current cathode material for solid oxide fuel cell (SOFC's) applications. Modifying the composition by adding Ca or Sr which substitute the La cations, leads to an enhancement of their electrical properties (2-4). Solid solutions based on another double oxides of manganese and light rare earth cations such as Pr, Nd and Sm, have also been studied as possible electrode materials for overcoming some inconvenient features of the lanthanum compounds (5).

The  $YMnO_3$  compound, and all the double oxides incorporating heavy rare earth cations, crystallise with a different hexagonal structure. Solid solutions of the type  $(Y_{1-x}Ca_x)MnO_3$  show a crystalline transition from hexagonal to a perovskite-type structure for Ca amounts higher than 20 at%. Below this amount two phases coexist: hexagonal and perovskite phases (6).

These perovskite-type solid solutions have adequate values of electrical conductivity and are an alternative for use as ceramic electrodes in SOFC's (7). Its compatibility with zirconia-type electrolytes is possibly higher than that of the lanthanum-calcium manganites.

The reasons for which the solid solutions  $(Y_{1-x}Ca_x)MnO_3$  show the phase transition are of two classes: the increase of the tolerance factor  $t=(r_A+r_O)/(r_B+r_O)^{1/2}$ , where  $r_A$  is the ionic radius in A sites,  $r_B$  is the ionic radius in B sites, and  $r_O$  is the ionic radius of the anion, (oxygen in this case), for the perovskite stability, due to the rise of the average ionic radius in A sites of the perovskite structure, when Ca, with ionic radius higher than that of Y, enters into the lattice, and the disappearance of the Jahn-Teller-type  $Mn^{3+}$  cations, some of them changing to  $Mn^{4+}$  to compensate the charge defect caused by the presence of  $Ca^{2+}$ (8)

Taking into account these reasons, it can be believed that the existence of solid solutions with perovskite-type structure of heavy rare earth manganites can be extended to other compounds, either by substituting the A cation by one with higher ionic radius, or by inducing the formation of  $Mn^{4+}$  cations on the B sublattice by substituting  $Mn^{3+}$  with appropriate cations of lower valence.

The main goal of the present work is to prepare and characterise the solid solutions whose general formula are the following:  $(Er_{1-x}Ca_x)MnO_3$  and  $Y(Ni_{1-x}Mn_x)O_3$ , in the Er and Mn rich regions respectively, and to correlate the obtained results with those corresponding to the better known  $(Yr_{1-x}Ca_x)MnO_3$ , and to the  $(Gd_{1-x}Ca_x)MnO_3$  solid solutions which is formed by two orthorhombic perovskites as end members.

## 2. EXPERIMENTAL METHODS

Reagent Grade oxides and Ca carbonate were used as raw materials for preparing the solid solutions. Manganese was incorporated as MnO compound, with >99,9% chemical purity, to ensure the correct Mn stoichiometry.

The weighed mixtures were thoroughly homogenised by attrition milling, preheated at 1150°C, remilled, pressed and sintered in air, from 1300 to 1400°C depending of each composition. The heating rate was 2°C/min, whereas the cooling rate was 1°C/min.

The sintered samples were grounded and milled for XRD analysis. The powders were mixed with Si which was used as the internal standard for measuring the lattice parameters. A diffractometer Siemens D-5000 was used for the analysis. CuK $\alpha$  radiation, filtered with Ni filter was employed for the phase identification, and the lattice parameter measurements. A scanning rate of 1/4 ° 2 $\theta$ /min was used, and 16 peaks, indexed according to the space group, (S.G). D<sup>16</sup><sub>2h</sub>-Pbnm were taken for the calculations. Minimum square fitting program was used, and a correlation coefficient >99,5% was established, with an error of  $\pm 0.0001$  nm. Values of the tolerance factor for the stabilisation of the perovskite-type structures are calculated using the ionic radii reported by Shannon & Pevitt, and corrected by O. Muller and R. Roy (9), under the hypothesis of the stoichiometric formula ABO<sub>3</sub>. It was also been supposed that the valence equilibrium between the different cations was established.

## 3. RESULTS

Table 1 summarises the crystalline parameters of the Gd-rich region of the pseudobinary GdMnO<sub>3</sub>-CaMnO<sub>3</sub> system. For all the compositions, complete solid solution was established. The most important effect is the lowering of the orthorhombicity factor b/a, i.e. the increase in the symmetry grade of the perovskite lattice, caused by a slight increase of the a parameter and a strong decrease of the b one. The structure evolves towards a quasi-tetragonal symmetry, with  $c/\sqrt{2}=a < b$ . Similar results were reported by Pollert et al. for the system Pr<sub>1-x</sub>Ca<sub>x</sub>MnO<sub>3</sub> in the 0.2  $\leq x \leq$  0.5 region. (8). The structural changes are attributed to the variation on the Mn<sup>3+</sup>/Mn<sup>4+</sup> ratio, which is induced by the presence of Ca<sup>2+</sup> cations substituting to Gd<sup>3+</sup>.

Figure 1 and Table 2 withdraw the results obtained on sam-

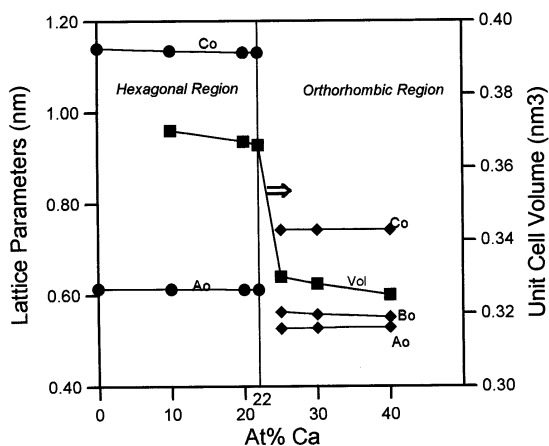


Figure 1.- Variation of lattice parameters and XRD density against the Ca amount in the (Y<sub>1-x</sub>Ca<sub>x</sub>)MnO<sub>3</sub> solid solutions

TABLE 1. LATTICE PARAMETERS OF THE SOLID SOLUTIONS GdMnO<sub>3</sub>-CaMnO<sub>3</sub>

At % Ca	a (nm)	b (nm)	c (nm)	b/a	V (nm <sup>3</sup> )
100/0	0.5313	0.5853	0.7432	1.102	0.231
80/20	0.5321	0.5640	0.7473	1.060	0.224
75/25	0.5320	0.5580	0.7480	1.049	0.222
70/30	0.5326	0.5558	0.7497	1.044	0.222
65/35	0.5326	0.5525	0.7515	1.037	0.221
60/40	0.5327	0.5482	0.7528	1.029	0.220

TABLE 2. LATTICE PARAMETERS OF THE SOLID SOLUTIONS Y<sub>1-x</sub>Ca<sub>x</sub>MnO<sub>3</sub>

AT % CA <sup>2+</sup>	a (nm)	b (nm)	c (nm)	b/a	V (nm <sup>3</sup> )	D <sub>t</sub> (g/cm <sup>3</sup> )
0*	0.6136	—	1.1400	—	0.372*	5.14
20*	0.6115	—	1.1303	—	0.366*	4.95
22*	0.6111	—	1.1255	—	0.364*	4.96
25	0.5272	0.5626	0.7427	1.067	0.220	5.42
30	0.5274	0.5584	0.7427	1.059	0.219	5.38
40	0.5300	0.5520	0.7427	1.042	0.217	5.27
50	0.5333	0.5410	0.7434	1.014	0.215	5.18

\* Hexagonal lattice, Z=6

ples belonging to the YMnO<sub>3</sub>-CaMnO<sub>3</sub> system. As it is already known (6) the Y-rich zone of the diagram shows two regions: the first one shows a hexagonal YMnO<sub>3</sub> solid solution, and for  $x \geq 0.22$  a transition to a single phase region, where an orthorhombic perovskite-type single phase structure takes place. The b/a ratio of the solid solutions is lowering with the increase of the Ca amount, in a similar manner to that observed in the Gd-Ca system. The most striking feature of these solid solutions is the strong increase of the XRD density, when the structure changes to the perovskite-type, despite of the lower atomic weight of Ca against Y. The structure of the perovskite solid solution with the lower Ca amount is similar to those described

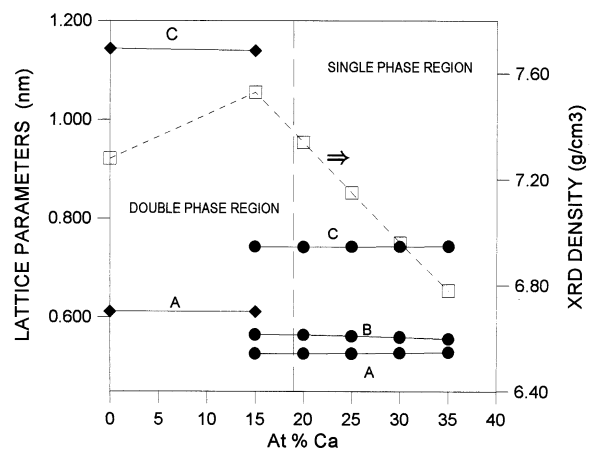


Figure 2.- Variation of lattice parameters and XRD density against the Ca amount in the (Er<sub>1-x</sub>Ca<sub>x</sub>)MnO<sub>3</sub> solid solutions

TABLE 3. LATTICE PARAMETERS OF SOLID SOLUTIONS  $Er_{1-x}Ca_xMnO_3$

AT % $Ca^{2+}$	a (nm)	b (nm)	c (nm)	b/a	V (nm <sup>3</sup> )	$D_t$ (g/cm <sup>3</sup> )
0	0.6117*	—	1.1435*	—	0.371*	7.28
15 <sup>#</sup>	0.5259	0.5647	0.7422	1.074	0.220	7.53
20	0.5262	0.5640	0.7418	1.072	0.220	7.34
25	0.5265	0.5618	0.7421	1.068	0.219	7.15
30	0.5275	0.5595	0.7425	1.061	0.219	6.96
35	0.5283	0.5558	0.7431	1.052	0.218	6.78

\* Hexagonal lattice, Z=6,

<sup>#</sup> Biphasic sample; lattice parameters correspond to the orthorhombic phase

TABLE 4. LATTICE PARAMETERS OF THE SOLID SOLUTIONS  $Y(Ni_xMn_{1-x})O_3$

At % Ni	a (nm)	b (nm)	c (nm)	b/a	V (nm <sup>3</sup> )	$D_t$ (g/cm <sup>3</sup> )
0	0.6136*	—	1.1400*	—	0.372*	5.15
20	0.5243	0.5651	0.7460	1.078	0.221	5.76
30	0.5241	0.5638	0.7452	1.076	0.220	5.82
33	0.5239	0.5641	0.7449	1.077	0.220	5.83
40	0.5229	0.5656	0.7427	1.082	0.219	5.85
45	0.5223	0.5666	0.7414	1.085	0.219	5.86
50	0.5221	0.5667	0.7412	1.086	0.219	5.87

\*Hexagonal Lattice, Z=6

above, with  $c/\sqrt{2} \approx a < b$ , called  $O'$  type elsewhere (8,10); when Ca amount increases the relation between the lattice parameters is being different:  $c/\sqrt{2} < a < b$ , (the so-called  $O$  structure), but with a trend of the a and b parameters. to be equalised.

Table 3 shows the results obtained from the solid solutions belonging to the  $ErMnO_3$ - $CaMnO_3$  system. As it can be seen, the behaviour has much similarities, but also depicts some differences, in respect to the Y system, even starting from a parent structure

In the same way as that of the previous Y system, there is a strong increase of the XRD density when the structure changes from hexagonal type to the orthorhombic one, (see value of the

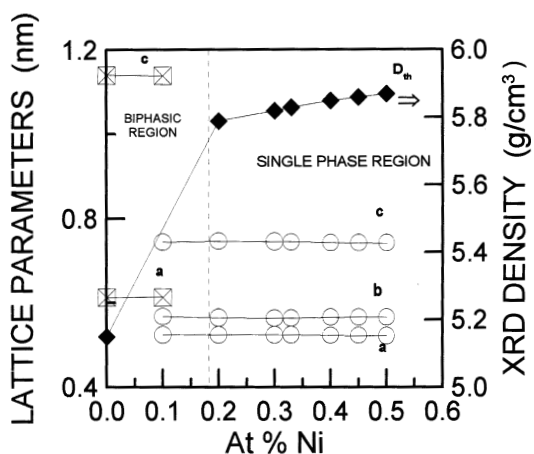


Figure 3.- Variation of lattice parameters and XRD density against the Ni amount in the  $Y(Ni_xMn_{1-x})O_3$  solid solutions

orthorhombic phase corresponding to 15 at% Ca, Table 3) which was also appreciated on the apparent density of the sintered samples. Further increase of the Ca amount causes a monotonous decrease of the XRD density. The transition from the biphasic to monophasic region is likewise present, but it occurs at a Ca amount lower than 20 at% Ca. The perovskite-type phase is parent to that of the Y system. Nevertheless, the variation of the b/a ratio is less pronounced, whereas the increase of the a parameter and the decrease of the b one are also less obvious. The 20 at% Ca composition show also a parameter relation of the type above described:  $c/\sqrt{2} \approx a < b$ . The rise on the Ca amount causes a slight lowering of the lattice volume. The perovskite-type phase corresponding to a 15 at% Ca, in the biphasic zone shows a lattice parameters very near to that of 20 at% Ca. Figure 2 shows a tentative phase diagram at room temperature based on the results obtained for this pseudobinary system.

Table 4 depicts the results obtained from the analysis of the compositions in the Mn-rich region of the  $Y(Ni_{1-x}Mn_x)O_3$  system. It can be seen that it also exists a crystalline transition from hexagonal to perovskite-type structure, located for a Ni amount of <20 at%, like that occurring in the Er system. At the same manner, the XRD density values show a strong increase from the hexagonal to the orthorhombic structure. Nevertheless, some differences can be appreciated: The XRD density rises monotonically until the composition with  $x=0.50$ . At the same time, the orthorhombicity factor, b/a grows with the amount of Ni. The c lattice parameter decreases slightly and the b and a parameters increases and decreases respectively, contrary to what was observed in the systems with modifications in the A sites, as the above described. The structure is near to that formed at low amount of Ca in the Y and Er systems,  $c/\sqrt{2} \approx a < b$ , but the parameter a is always lower than the  $c/\sqrt{2}$ , whereas the value of b is higher than a and  $c/\sqrt{2}$ , in the whole compositional range studied.

On the other hand, compositions with  $x > 0.50$  at% Ni have shown to be biphasic: presence of free  $Y_2O_3$  has been detected, indicating that the  $Ni^{2+}$  did not passed to  $Ni^{3+}$ , in the present processing conditions, to form a perovskite structure with a valence distribution of the type  $Y(Ni^{3+}_{2x-1}Ni^{2+}_{1-x}Mn^{4+}_{1-x})O_3$  ( $x > 0.50$ ) as would correspond to a valence equilibrium, taking as hypothesis the correct stoichiometry of the oxygen in the general formula  $ABO_3$ . This behaviour is similar to that described for the  $NiO$ - $La_2O_3$  system, in which the thermal stabi-

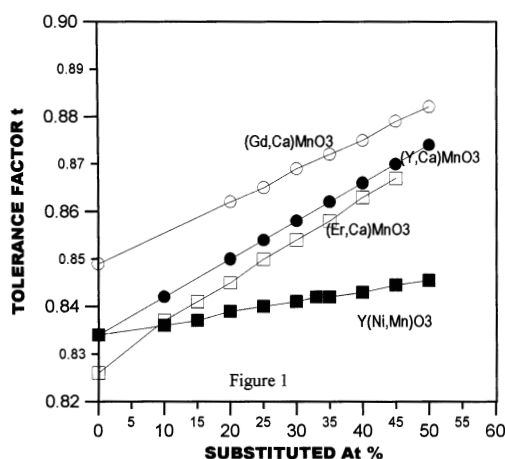


Figure 4.- Tolerance factor t vs x for the different solid solutions series

lity range of existence for the  $\text{LaNiO}_3$  perovskite-type compound is very narrow and it decomposes giving  $\text{NiO}$  and  $\text{La}_2\text{NiO}_4$  compounds (11). Figure 3 is a tentative room temperature phase diagram for the present system.

#### 4. DISCUSSION

The existence of hexagonal structures in heavy rare earth and Y manganites is explained by the confluence of two factors. The decrease of the ionic radius of the lanthanides with the rise of the atomic number leads to a lowering of the perovskite lattice stability. This stability is governed by the tolerance factor  $t$ . On the other hand, the lanthanide manganites incorporate in the lattice  $\text{Mn}^{3+}$  Jahn-Teller-type cations. These cations have a great capacity to adopt a fivefold trigonal bipyramidal co-ordination. This ability explains the high orthorhombic factor values of some light lanthanide manganites, such as the Gd manganite. When the tolerance factor falls below a given value, the combination of both effects leads to the appearance of a new type of structure, strongly oriented according to a preferential axis.

The substitution of Y or Er by Ca increases the average ionic radius of the A sites, and therefore the tolerance factor is being also increased. At the same time, one part of the  $\text{Mn}^{3+}$  cations must pass to a higher valence state  $\text{Mn}^{4+}$  to compensate the lower valence of Ca against the Y or Er (6). This weakens the cooperative Jahn-Teller effect and therefore induces the transition to the perovskite structure (8). The presence of the  $\text{Mn}^{4+}$  causes a shortening of the octahedra which explains the increase of the XRD density. It is interesting to consider that the presence of  $\text{Mn}^{4+}$  also contributes to the rise of the tolerance factor.

A different, non-referred case is that of the solid solutions  $\text{Y}(\text{Ni},\text{Mn})\text{O}_3$ . The ionic radius of the  $\text{Ni}^{2+}$  is somewhat higher than that of the substituted  $\text{Mn}^{3+}$  and, therefore, the tolerance factor  $t$  must be decreased. On the other hand, the presence of  $\text{Mn}^{4+}$  induced by the  $\text{Ni}^{2+}$ , and confirmed by the increase of the electrical conductivity (11) lowers the average ionic radius of the B sites and can counteract the effect induced by the Ni ion.

Figure 4 depicts the variation of the tolerance factor,  $t$  against the  $x$  value, independently of the substituted lattice site. The calculation of  $t$  of these solid solution series shows a slight increase of  $t$  with the amount of Ni cation. Values of  $t$  corresponding to the first compositions with the perovskite structure:  $x=0.20$  and  $0.30$  at% Ni, are lower than those which theoretically would correspond to the solid solutions of the

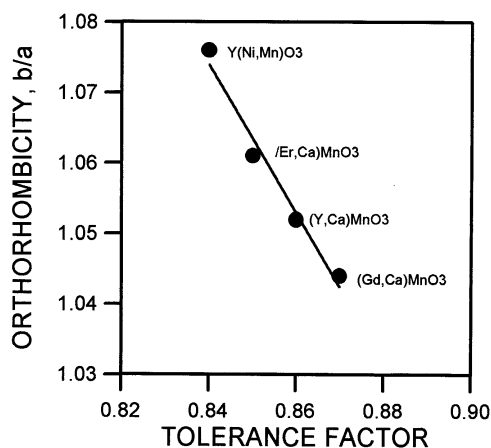


Figure 5.- Orthorhombicity factor,  $b/a$  against tolerance factor  $t$  for the different solid solutions with the same  $x=0.3$

$(\text{Y,Ca})\text{MnO}_3$  system with  $x=0.10$  and  $0.20$  in which the hexagonal structure is maintained. It is possible to state that the presence of Jahn-Teller cations in the manganites lattice is more relevant than the value of the tolerance factor  $t$  to explain the crystalline structure adopted for each manganite composition.

The low values of  $t$  calculated for the  $\text{Y}(\text{Ni},\text{Mn})\text{O}_3$  solid solutions are the cause of the high orthorhombicity character of the perovskite structure. It must be taken into account that the incorporation of a Ni cation induces the formation of two  $\text{Mn}^{4+}$  ions instead of one, as it is in the case of the A-substituted Y or Er manganites. Therefore the predominant mechanism for crystallisation in one of the forms  $O$ , or  $O'$  is the steric effect associated to the tolerance factor, which in this case leads to the  $O$  type form, with  $b > c/\sqrt{2} > a$ , and an orthorhombicity factor corresponding to values near that of the stability limit.

Figure 5 shows the relation between the tolerance factor  $t$  and the orthorhombicity ratio  $b/a$ , for a set of samples with the same amount (30 at%) of the modifying cation. It can be seen a good correlation which exists between both parameters, independent of the chemical composition of the perovskite-type solid solutions.

#### 5. CONCLUSIONS

A new family of solid solutions with perovskite structure, based on modified  $\text{RE}\text{MnO}_3$  ( $\text{RE}=\text{Er}, \text{Y}$ ), hexagonal manganites, with  $\text{Ca}^{2+}$  and  $\text{Ni}^{2+}$  modifying cations in A or B sites of the manganites lattice, is described.

The formation of the perovskite phases depends not only on the tolerance factor value,  $t$ , but also on the  $\text{Mn}^{3+}/\text{Mn}^{4+}$  ratio, modified by the presence of the aliovalent cations. The existence of the crystalline transition is independent of the lattice site where the substituting cation enters.

#### ACKNOWLEDGEMENT

This work was supported under contract CICYT-MAT-97-0679-C02-01

#### 6. REFERENCES

1. N.Q. Minh "Ceramic Fuel Cells", J. Amer. Ceram. Soc., **76**, 563-588, (1993)
2. J.H. Kuo, H.U. Anderson, D.M. Sparlin, "Oxidation-Reduction behaviour of undoped and Sr-doped  $\text{LaMnO}_3$ : Defect structure, Electrical conductivity and thermoelectric power" J. Solid State Chem **87**, 55-63, (1990)
3. A. Hammouche, E. Siebert, A. Hammou, "Crystallographic, thermal and electrochemical properties of the system  $\text{La}_{1-x}\text{Sr}_x\text{MnO}_3$  for high temperature Solid Oxide Fuel Cells" Mater. Res. Bull., **24**, 367-80, (1989)
4. J. Tanaka, K. Takahashi, K. Yukino, S. Horiuchi, "Electrical conduction of  $(\text{La}_{0.8}\text{Ca}_{0.2})\text{MnO}_3$  with homogeneous ionic distribution" Phys. Status Solidi, **80**, 621-630, (1983)
5. H. Taimatsu, K. Wada, H. Kaneko, "Mechanism of reaction between Lanthanum Manganite and Yttria-stabilized Zirconia" J. Amer. Ceram. Soc., **75**, 401-405, (1992)
6. C. Moure, M. Villegas, J.F. Fernandez, P. Duran, "Phase transition and electrical conductivity in the system  $\text{YMnO}_3\text{-CaMnO}_3$ ", J. Mater. Sci. **34**, 2565-2568, (1999)
7. J.W. Stevenson, M.M. Nasrallah, H.U. Anderson, D.M. Sparlin, "Defect structure of  $\text{Y}_{1-x}\text{Ca}_x\text{MnO}_3$  and  $\text{La}_{1-x}\text{Ca}_x\text{MnO}_3$ ", J. Solid State Chem. **102**, 175-197, (1993)
8. E. Pollert, S. Kupriska, E. Kusmicova, "Structural Study of  $\text{Pr}_{1-x}\text{Ca}_x\text{MnO}_3$  and  $\text{Y}_{1-x}\text{Ca}_x\text{MnO}_3$  perovskites", J. Phys. Chem. Solids, **43**, 1137-1145, (1982)
9. O. Muller, R. Roy, p.5-7 "The Major Ternary Structural Family", Springer Verlag, N.Y. (USA) 1974,
10. G.Ch. Kostoglouidis, Ch. Ftikos, "Effect of Sr-doping on the structural and electrical properties of gadolinium manganite oxide", J. Mater. Sci., **34**, 2169-73, (1999)
11. D. Gutierrez, J.F. Fernandez, P. Duran, C. Moure, "Crystalline structure and electrical properties of solid solutions  $\text{YNi}_x\text{Mn}_{1-x}\text{O}_3$ ". Bol. Soc. Esp. Ceram. Vidrio **38** [6] (1999) (en prensa).